isvr Institute of Sound and Vibration Research

Low Frequency Airborne Sound Transmission in Buildings: Modal Analysis (Computational Experiments)

M.D.C. Magalhaes and N.S. Ferguson

ISVR Technical Memorandum 853

October 2000

University of Southampton

SCIENTIFIC PUBLICATIONS BY THE ISVR

Technical Reports are published to promote timely dissemination of research results by ISVR personnel. This medium permits more detailed presentation than is usually acceptable for scientific journals. Responsibility for both the content and any opinions expressed rests entirely with the author(s).

Technical Memoranda are produced to enable the early or preliminary release of information by ISVR personnel where such release is deemed to the appropriate. Information contained in these memoranda may be incomplete, or form part of a continuing programme; this should be borne in mind when using or quoting from these documents.

Contract Reports are produced to record the results of scientific work carried out for sponsors, under contract. The ISVR treats these reports as confidential to sponsors and does not make them available for general circulation. Individual sponsors may, however, authorize subsequent release of the material.

UNIVERSITY OF SOUTHAMPTON

INSTITUTE OF SOUND AND VIBRATION RESEARCH

DYNAMICS GROUP

Low Frequency Airborne Sound Transmission in Buildings: Modal Analysis

(Computational Experiments)

by

M.D.C. Magalhaes and N.S. Ferguson

ISVR Technical Memorandum No. 853

October 2000

Summary

This report describes the general theoretical model for interior sound fields, which are created by excitations of coupled systems due to a noise source.

The pressure is explicitly described in terms of the modal parameters and structural-acoustic modal coupling coefficients, which have a large effect on the noise reduction values at the resonant frequencies.

Numerical predictions are presented considering the governing equations for general acoustic-structural coupled systems. These procedures were evaluated by using a computer program, which has been developed during the course of this study in MATLAB. Simulations show the effect of several configurations for a flexible partition (different geometric arrangements in the wall) and for the rooms (size and absorbing walls), on the noise reduction parameter.

In addition, transmission loss for the models, obtained via modal analysis, are compared with those obtained by conventional approaches.

Contents

1 Introduction

The initial aim of this work is to improve the understanding of the noise transmission phenomenon in buildings, at low frequencies, under conditions of an acoustic-structural coupled room-plate-room model. This has been represented by sets of integro-differential modal equations of motions. Furthermore, the low-frequency range has been defined as the modal domain, for which the associated conservative system has a low modal density [9]. The effects of low-frequency noise has been of a particular concern because many kinds of structures has been inefficient in attenuating low-frequency noise, compared to other frequency components.

The frequency range of human hearing is considered to be between 20 Hz and 20,000 Hz. However, it has been shown that humans can not only perceive a sound below 20 Hz (if one considers a signal that has a high sound pressure level) but also detect it through their bodies [6].

For this report, a third octave band up to 250 Hz is considered.

Sound insulation requirements in buildings depend on the listener's activities and also on the background noise, which may be considered as part of the work environment. The problem of sound transmission has become an important subject in noise control in buildings. Usually, a noise is communicated to rooms via many different paths. Moreover, noise sources may be elsewhere in the building and/or outside the building. In airborne sound transmission the noise originates in the air. This work considers the insulation provided by a single-leaf partition against airborne sound. The greater the sound insulation provided by a partition, the higher its sound reduction index.

The problem of calculating the sound transmission between rooms has been investigated over many years [1,2,3,4,16,19]. The three main approaches have been the conventional Wave Approach, Modal Analysis and Statistical Energy Analysis.

In the Wave Approach, infinitely extended panels are used as sound transmission models. For the first group of these models, boundary effects are neglected and the walls are assumed to be homogeneous and to have no leaks. The so-called mass law behaviour has been successfully applied to many situations where frequencies are well below the coincidence frequency. However, the assumptions provided are unsatisfactory in a large number of real panels whose dimensions are less than or equal to the wavelength of the incident sound wave. In addition, the geometry of the system is not taken into account.

On the other hand, The Modal Analysis allows the introduction of geometric parameters of the system, in the rooms and common wall, to be incorporated in the models and subsequent predictions. The frequency response of a finite-system normally has peaks and dips, due to the resonance phenomenon involving modal behavior and fluid-structure spatial coupling of plate and room modes. This method also permits one to calculate radiation of small structures at low frequencies, within a reasonable operational running time.

Finally, Statistical Energy Analysis considers the power flow balance between linear coupled systems. Statistical energy Analysis (SEA) has been applied to solve some problems of noise transmission in buildings, aircraft, cars, etc. The estimates of subsystem energies are obtained on the basis of known 'a priori' values for the loss factors, coupling loss factors and the power inputs [9].

Effects of panel boundaries on the sound transmission, including a comparison with an infinite panel, have been discussed in ref. [16]. A simple two-dimensional model was used for evaluating the sound transmission characteristics of finite panels. The effects of the panel size were verified in regions below, above and at the critical frequency. Estimates of averaging the response over a particular frequency range have also been presented.

There has also been further investigation, [1], with work closely related to this research. The transmission of a reverberant sound field through a rectangular baffled partition, by

means of a mode expansion method, was analyzed. According to the formulae, valid for non-resonant transmission, the problem was well predicted provided that the mass of the partition was significant. In those conditions, it pointed out that the imaginary part of the fluid wave impedance is significantly greater than its real part. Therefore it ensured that the forced vibration, or *mass law* contribution, dominated the transmission factor.

A detailed review of interior sound field problems has also been presented by Dowell et al [1] in order to investigate acoustic-structural coupled systems. In his work, a theoretical model was developed for arbitrary wall motions by using Green's Theorem. From the point of view of applications, a simplified formulation was also presented for sound level predictions in terms of acoustic and structural parameters.

Takahashi [17] has discussed the effects of the finite size of a panel on the sound transmission, in comparison with the infinite panel theory. The analysis of the transmission, through a baffled plate of finite width and infinite length, was conducted rigorously. Sound transmission in the diffuse field was hence obtained via numerical direct-integration.

More recently, Osipov et al [18] has evaluated some numerical examples in order to verify the influence of the dimensions of rooms and partitions on transmission phenomenon. The problem of low frequency sound insulation in buildings was identified as a growing researching area. In his work, three distinct theoretical models (infinite plate theory, modal analysis for a baffled partition and for a room-plate-room system) were compared with experimental results.

In ref. [21], sound insulation has also been predicted by using modal analyses. However, that model did not include the resonant behavior of the partition. The partition only represented a connection between both rooms, instead of a resonant subsystem. Recently, in ref. [22], Finite Element Method has also been used to predict the sound insulation considering the effect of partition edge conditions at low frequencies. Furthermore, an

interesting approach, considering impedance-mobility representations, has been adopted and applied to many sound and vibration problems [3].

In summary, a vast amount of research concerning with the acoustic-structural coupling has been published. The literature survey has shown that a large amount of work has been performed in the analysis of sound insulation phenomenon. However, the combined effect of parameters in noise control in buildings has not been fully explored yet. With a point noise source placed in either of the rooms, the aim is to predict the noise reduction of the system due to resonant coupling involving modal behaviour, spatial fluid-structural coupling and non-resonant contributions. Moreover, some interesting results in terms of transmission efficiency are examined when the weight of the partition is increased. The transmission of sound through corridors is also predicted in this research. A study of the influence of system dimensions on the insulation [18] is made by averaging over 1/3 octave bands. An analysis of the position or arrangement of a flexible panel in the common wall, considering that all other parts of the common wall are rigid, is predicted. Finally, a general discussion, based on the findings of the results obtained, is presented.

2 Theoretical Background of Sound Transmission Mechanism

The noise control engineer for buildings has often been faced with the problem of specifying wall materials, type of partition mountings and suitable technique of construction to be used in the insulation of rooms. The most common problem has been transmission of sound through solid partitions such as walls, windows, floor, etc.

Mechanism of transmission may be characterised by a radiated sound field from a elastic partition. The response of thin plates to localised excitation results in free bending waves. Those waves interact with plate edges producing sound power radiation. In addition, another contribution to the total radiated noise comes from the in phase vibration of the plate in the vicinity of the excitation point. On the other hand, when a sound wave is incident upon a partition, the response, which is frequency dependent, is also dependent on the radiation impedance of the modes of the partition. Thus, the air on the other side of the plate is excited, and a sound wave is then propagated into the receiving volume.

In general, the sound transmission theory for uniform and unbounded panels has widely been used to approximate the sound transmission loss of a bounded panel in a baffle. Of course, some assumptions, such as random-incidence field over the partition, as well as a limited frequency range (in which the acoustical wavelength is smaller than the plate size), have been considered.

A transmission efficiency parameter τ defined as the ratio of transmitted to incident power, is given by

$$\tau = \frac{W_{trans}}{W_{inc}} \tag{2.1}$$

where: $\mathbf{w}_{\mathbf{trans}}$ is the transmitted sound power;

$\mathbf{w}_{\mathbf{inc}}$ is the sound power incident on the source side of the test partition.

A classical index, known as Transmission Loss (TL), in some countries, or Sound Reduction Index (SRI) has also been defined as

$$\mathrm{SRI} = 10 \log_{10} (1/\tau) \ \ (\mathrm{dB}) \tag{2.2}$$

A finite-size panel (bounded rectangular plate in a baffle) is a more realistic model than the infinite one described above. The transmission is characterized by boundary effects, which lead to form standing-wave modes. Simple supported edges will be considered for a rectangular plate of length L_z and width L_y.

An infinite set of *in vacuo* modes, represented by a functional basis, which is assumed to be the solution of the equation of motion for the flexible plate, is given by

$$\phi_p(z,y) = \sin(k_z z)\sin(k_y y) \tag{2.3}$$

This basis function, used in the expansion for the panel deflection, must not only ensure a vanishing normal displacement on the contour of the panel but also respect the panel boundary conditions. It satisfies the boundary conditions and the equation of motion as long as

$$k_b^2 = k_{pr}^2 = \left(\frac{r\pi}{L_Z}\right)^2 + \left(\frac{s\pi}{L_y}\right)^2 \tag{2.4}$$

where $(k_{pr})^2$ – *in vacuo* eigenvalues

L_z – length of the panel;

L_y – height of the panel;

r, s – panel mode;

Furthermore, the infinite set of modes, defined by Equation 2.3, represents a set of orthogonal functions, which satisfy the relations

$$\begin{aligned} \int_S m(r_s)\phi_q\phi_p \, dS &= \begin{cases} 0 \ if \ p \neq q; \\ \Lambda_p \ if \ p = q. \end{cases} \\ \Lambda_p &= \int_S m(r_s)\ \phi_p^2 \, dS \end{aligned} \tag{2.5}$$

where $m(r_s)$ = mass/unit area of the partition.

To determine the far-field sound intensity radiated and consequently the transmission, one has to evaluate the sound field generated by a harmonic vibrating surface. The sound field, generated by a harmonic vibrating surface **S** at position **r** in the fluid, is given by a particular form of Kirchhoff-Helmholtz integral equation, which is termed Rayleigh Integral [4]. The key function of this problem is to obtain the difference of pressure between both sides of the panel.

The total surface pressure is hence the summation of the *blocked pressure* and the radiated pressure. This *blocked pressure* is defined as the summation of the incident field and the scattered field, produced if the plate were rigid (infinite mechanical impedance). The radiated pressure is the field produced as a result of the elasticity of the plate. Therefore, only the radiated field contributes to the total surface velocity of the plate.

At first, one has to solve the equation of motion of an elastic partition defined as

$$D\left\{\nabla^4[w(z,y,\omega)]-k_b^4\, w(z,y,\omega)\right\}= F_{bL} \tag{2.6}$$

and

$$w(z,y,\omega)=\sum_p w_p\phi_p \tag{2.7}$$

$$F_{bL}=2\int_S F_o\phi_p\, dS \tag{2.8}$$

where F_{bL} - blocked pressure;

F_o – incident field amplitude;

ϕ_p – basis function;

D – bending stiffness;

∇^4 – square of the Laplace operator;

k_b – wavenumber of the free-bending wave;

w(z, y, ω) – normal displacement of the plate surface;

In Equation 2.6 the time term $e^{j\omega t}$ is suppressed, as well as the damping influence. After solving this equation, the power radiated into a half-space, due to the plate vibration, can be obtained by

$$\prod(\omega) = \frac{1}{2}\int_S \mathrm{Re}\left[p(z,y,0)\, \dot{w}(z,y,0) \right] dS \tag{2.9}$$

The real part of the radiation impedance (radiation resistance) may be also defined for the **p** mode of the plate as

$$R_p = \frac{\prod(\omega)}{\frac{1}{2}\left\langle \left| \dot{w}_p \right|^2 \right\rangle} \tag{2.10}$$

where the spatial average mean square normal velocity is given by

$$\left\langle \left| \dot{w}_p \right|^2 \right\rangle = \frac{1}{S}\int_S \left| \dot{w}_p \right|^2 dS \tag{2.11}$$

Finally, the full problem, considering the fluid loading in the equation of motion, can be solved. Thus, one may obtain some results in terms of coupled *in vacuo modes.*

Let p(x,y,z,t) be regarded as small amplitude pertubation (acoustic pressure variation), from its equilibrium value. The wave equation, which results from the linear acoustics equations, is given by [6]

$$\begin{aligned} &\nabla^2 p - \frac{1}{c^2}\frac{\partial^2 p}{\partial t^2} = 0 \\ &\frac{\partial p}{\partial n} = 0 \text{ on the rigid walls of the room;} \\ &\frac{\partial p}{\partial n} = -\rho_o \frac{\partial^2 w}{\partial t^2} \text{ on the flexible partition} \end{aligned} \tag{2.12}$$

where w = The displacement of the flexible partition in the normal direction (positive outward).

The steady-state solution is obtained through the Fourier Transform of the time domain wave equation. Hence, it yields the Helmholtz Equation

$$\nabla^2 \bar{p} + k^2 \bar{p} = 0 \tag{2.13}$$

If $\bar{p}$ is expressed as an expansion of eigenfrequencies for the room, corresponding to the resonances of a rigid boundary space, a Green's Function can be obtained satisfying the same condition [4]

$$\frac{\partial G(r \mid r_o)}{\partial n} = 0 \qquad r \in S_r$$
$$\nabla^2 G(r \mid r_o) + k^2 G(r \mid r_o) = -\delta(r - r_o) \tag{2.14}$$

where S_r is the surface area of the rigid walls;

$-\delta(r - r_o)$ is the three-dimensional Dirac Delta function representation of a point source.

The spatial form for the three-dimensional eigenfunctions ψ_n, corresponding to the natural frequency ω_n of the rigid-walled space, may be defined as

$$\Psi_n = \cos\left(\frac{n_x \pi . x}{L_x}\right) \cos\left(\frac{n_y \pi . y}{L_y}\right) \cos\left(\frac{n_z \pi . z}{L_z}\right) \tag{2.15}$$

This set of modes satisfy the relation

$$\int_S \psi_m \psi_n \, dS = \begin{cases} 0 \ if \ m \neq n; \\ \Lambda_n \ if \ m = n. \end{cases}$$
$$\Lambda_n = \int_V \psi_n^2(x, y, z) \, dV \tag{2.16}$$

Since ψ_n is an eigenfunction of the room, it has a correspondent eigenvalue k_n which must satisfy

$$\nabla^2\Psi_n + k^2\Psi_n = 0 \tag{2.17}$$

Therefore, using the previous relationships, equation (2.14) can be written as

$$\sum_n A_n(-k_n^2 + k)\Psi_n = -\delta(r - r_o) \tag{2.18}$$

Multiplying each side of equation (2.18) by $\psi_m(x,y,z)$ and integrating over the volume of the room one has [4]

$$A_n = \frac{\Psi_n(x_0, y_0, z_0)}{A_n(k_n^2 - k^2)} \tag{2.19}$$

A review of velocity-potential concepts is also important if one uses an alternative formulation. For an inviscid-flow (viscous effects are neglected), low-speed flows are irrotational [15]. It means that

$$\begin{aligned} &\text{If} \nabla V \equiv 0 \quad \text{then} V = \nabla\Phi \\ &u_x = \frac{\partial\Phi}{\partial x};\ u_y = \frac{\partial\Phi}{\partial y};\ u_z = \frac{\partial\Phi}{\partial z}; \end{aligned} \tag{2.20}$$

where V fluid velocity;

(u_x, u_y, u_z) fluid velocity components;

Φ - scalar function termed velocity potential.

Therefore, the velocity potential function allows one to obtain all other acoustic parameters through the relation

$$p = -\rho_o \frac{\partial \Phi}{\partial t} \tag{2.21}$$

Beranek [2] has suggested a simple formulation, in which the sum of the radiation efficiency (in dB) of the sound-forced finite plate plus 3 dB, is subtracted from the value obtained by normal incidence mass-law. In this approximation, the radiation efficiency used was originally defined in ref. [16].

The transmission loss for a baffled panel has also been studied by Leppington [11]. His predictions have been considered an improvement on previous theories. A random field was considered as an infinite sum of uncorrelated plane-waves impinging on the finite-panel surface. In contrast, an assumption, that has been usually adopted, was to consider the random field as a diffuse field, neglecting the presence of the boundaries. Moreover, the transmission problem was described in terms of two distinct mechanisms.

The first one is dominant at the region of the spectrum above the critical frequency, where free bending waves interact to cause resonance. In this frequency range, the partition is a good radiator. In fact, its radiation efficiency is always greater than or equal to the unity. The fundamental mode is an exception because it is strongly excited at a frequency equal to zero.

For the second mechanism, free bending waves are not generated, and in this frequency range (below the critical frequency), the partition behaviours as a poor radiator.

In summary, one can consider the transmission phenomenon as a summation of the non-resonant transmission or forced transmission, and the resonant transmission. In numerous cases, the resonant transmission for frequencies below the critical frequency of the partition has been ignored [10,11].

3 Theoretical Model for the Fluid-Structural Coupled System

In the present analysis, the room-panel-room system is selected as the fundamental model, which may represent a real situation in a building. The physical mechanisms involved in the control of sound transmission in buildings can be hence evaluated. As mentioned previously, the analytical modal model adopted [4] is based on a set of integro-differential equation formulation of the interaction between a flexible plate and enclosed fluids. The acoustic and the structural fields are expressed in terms of their uncoupled modes by means of differential equations for each mode. Therefore, the structural motion has been expressed as a summation over the response in the *in- vacuo* natural modes driven by a fluid loading. The acoustic-field of the rigid-walled rectangular rooms has been determined by the summation of the acoustic modes over the fluid volume. In fact, these acoustic modes were excited by a generalized volume velocity (whose value was set equal to unit) inside the source room.

The interaction analysis has been conducted as two fluid volumes bounded by a thin plate were excited as a point monopole source was placed in one of them. In addition, solid surfaces, which bounded volumes of air V_1 and V_2, were considered. The response of the coupled system to a forcing harmonic function has been given in terms of the uncoupled modes of both rooms and the uncoupled panel modes by Fahy [4]:

$$\begin{aligned}
&\ddot{\Phi}_{n1} + \beta_{n1}.\dot{\Phi}_{n1} + \omega_1^2\,\Phi_{n1} = (c^2 S/\Lambda_{n1})\sum_p \dot{w}_p .C_{n1p} - c^2 Q_{n1}/\Lambda_{n1} \\
&\ddot{w}_p + \beta_p.\dot{w}_p + \omega_p^2.w_p = -(\rho_o.S/\Lambda_p)\sum_{n1}\dot{\Phi}_{n1}.C_{n1p} + (\rho_o.S/\Lambda_p)\sum_{n2}\dot{\Phi}_{n2}.C_{n2p} \qquad (3.1) \\
&\ddot{\Phi}_{n2} + \beta_{n2}.\dot{\Phi}_{n2} + \omega_2^2.\Phi_{n2} = -(c^2 S/\Lambda_{n2})\sum_p \dot{w}_p .C_{n2p}
\end{aligned}$$

where indices $\mathbf{n_1}$, $\mathbf{n_2}$, and $\mathbf{p}$ refer to source room, receiver room and panel modes respectively;

The spatial structural-acoustic coupling coefficient $\mathbf{C_{np}}$ is defined by

$$\frac{1}{S}\int_S \psi_p.\phi_n dS \qquad (3.2)$$

where simply-supported edges are assumed for the partition

Q = generalized volume velocity,

Φ = modal velocity potential amplitude,

β = generalized modal-damping coefficient.

The determination of the coupled modal frequencies and their eigenfunctions have been evaluated numerically by using a dynamics matrix formulation for the eigenvalue problem. The analysis was applied to the free vibration problem of the coupled room-panel-room system in order to determine the eigenvalues and eigenvector, and also to the forced-vibration problem.

Hence, an average absorption coefficient was firstly considered in terms of the corresponding modal loss factor. Then, spatial averaged mean square pressures, whose amplitudes have been obtained directly from the linear plate equation and velocity potential equations for the rooms, are also calculated.

The transmission parameters obtained from modal room-panel-room model, finite-panel predictions [1,11] and a classical approach are compared graphically as a function of frequency.

The 'loading', applied to the source room, is represented by the generalized source strength as [3]

$$Q_n = \int_V q_o \Psi_n(x, y, z)\, dV \tag{3.3}$$

where q_o = source volume velocity per unit volume.

In equation 3.1, the effect of the absorbing material has been approximated by equivalent damping factors β_n.

Neglecting the cross-modal coupling terms, introduced by the absorption on the boundary of the volume, and assuming that a single room mode is dominant, the approximation for the generalized modal damping may be given by [1]

$$\beta_n = \left(\frac{\rho_o c^2}{\Lambda_n} \right) \int_A \frac{\psi_n \psi_n}{z_a} dA \tag{3.4}$$

The real specific acoustic impedance z_a for the wall surfaces, lined by a soft blanked, on the assumption of neglecting its imaginary part and the reflected sound waves in the layer , may be approximated by [18]

$$z_a = \frac{8 \rho_o c}{\alpha} \tag{3.5}$$

where α is the diffuse absorption coefficient for an internal surface A of the room.

The pressure field, which acts on the partition surface, may be expressed in the acoustic and structural basis. At any particular point on the plate, the pressure values obtained from either the acoustic or structural basis function expansion are equal. Therefore, the generalized force exerted on the p^{th} plate mode by the n^{th} acoustic mode of the receiving room is expressed as [18]

$$F_n^R = \frac{C_{n2p}}{\Lambda_p} p_{n2} \tag{3.6}$$

where

p_{n2} = the receiving room modal pressure.

C_{n2p} = geometrical coupling coefficients between the panel modes and the receiving room modes.

The spatial-averaged mean normal intensity transmitted by the panel is defined as [12]

$$< I_R > = \frac{1}{S} \int_S Re\{F_n^R v^*\} dS \tag{3.7}$$

where v^* = complex conjugate of the particle velocity at panel boundary;

F_n^R = r.m.s. pressure over the partition in the receiving-room.

As the particle velocity is equal to the normal velocity of the panel on its surface, the previous equation was hence evaluated as

$$< I_R > = \frac{1}{S} \sum_p \mathrm{Re}\left\{ F_n^R . \dot{w}^* \right\} \Lambda_p \tag{3.8}$$

Therefore, according to equation 3.6 the transmitted intensity can be expressed as

$$< I_R > = \frac{1}{S} \sum_p \sum_n \mathrm{Re}\left\{ C_{n2p} . p_{n2} . \dot{w}_p^* \right\} \tag{3.9}$$

The mean sound intensity incident on the partition has been approximated by the potential energy in the source room due to the modal density. Finally, one can evaluate the SRI (Sound Reduction Index) and the NR (Noise Reduction) as

$$SRI = 10 \log_{10} \left(\frac{\left\langle |p_{n1}|^2 \right\rangle}{\rho_o c < I_R >} \right) \tag{3.10}$$

and

$$NR = 10 \log_{10} \left(\frac{\left\langle |p_{n1}|^2 \right\rangle}{\left\langle |p_{n2}|^2 \right\rangle} \right) \tag{3.11}$$

The theoretical routines were developed according to the chart below:

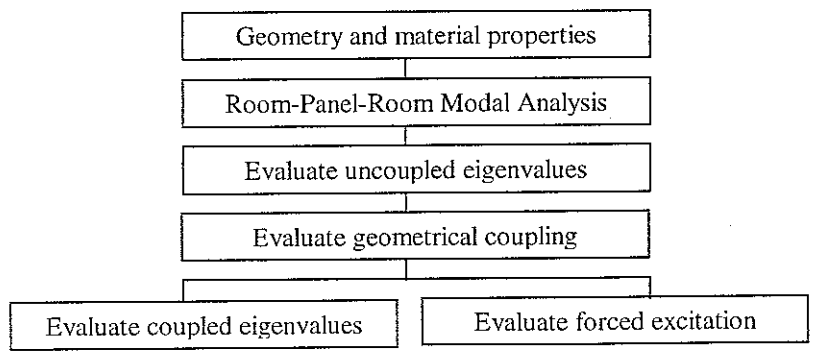

4 Numerical Results

4.1 – General description of models

The models adopted have been composed by three subsystems: a source room, a common wall and a receiving room. The source room was defined as an acoustic volume excited by a broadband acoustic point source placed in a specific position, and the receiving room defined as the acoustic volume connected to the source volume through a common rigid wall with a flexible elastic portion. The results obtained from numerical examples have provided important information about the sensitivity of the Sound Reduction Index to some parameters not normally considered in design of buildings. The details of the models are shown in Figure 3.

The system properties are described as follows. For a partition made of plasterboard material, a value of $\upsilon = 0.2$ and $E = 2.12E9$ (N/m^2) were adopted for Poisson's ratio coefficient and Young's Modulus respectively. Also, density value of $\rho_s = 806$ (kg/m^3) and thickness of 0.025 (m) were assumed for the material. The thickness chosen corresponds to about 1/7 the wavelength of the highest frequency of interest (350 Hz). Therefore, the assumption of only pure bending waves propagating in the panel remains valid.

When varying the other parameters, the receiving and source room surfaces were considered covered by a soft material with a constant modal frequency-averaged damping of 5%. Nevertheless, as mentioned previously, an important approximation considered here is that the mode functions have been defined to be used as the mode shapes of a volume bounded by rigid walls.

Moreover, the acoustic source strength applied to the source room was unit volume velocity (1 m^3/s). It was placed at the position 1 (corner of the room) for all simulations other than that one for analyzing the influence of source position on SRI obviously.

It may be verified that the location of the resonance peaks and dips, for the harmonic forced response, coincided with the eigenvalues obtained from the coupled analysis. For the panel dimensions 2x5 m^2 and 2x2 m^2, a total of 133 and 52 modes were considered respectively. For the room dimensions 2x2x5 m^3 and 2x2x2 m^3 130 and 53 modes were obtained respectively (uniform pressure mode not included).

The results show that strongly excited structural modes generate low values for the SRI, which were determined by the structural-acoustic modal coupling coefficients as well as the damping factors. It is also noted (see tables 2 and 3) that the absorbing material and the internal loss factor of the plate had a little effect on shifting the eigenfrequencies, whereas the geometrical coupling coefficients played a leading role.
Another important point is that for the model 1, resonance frequencies of the panel (1x1 m^2) were greater than the resonance frequencies of the rooms. In that situation, the room modes contributed an equivalent stiffness. Also, it is noted (see table 4) that the lowest structural mode was most affected by the rooms.

For the system used in this study, all modes in the frequency range up to 350Hz have been included. Although some simplification due to the 'poor' spatial structural-acoustic coupling of the higher order modes, has been suggested by some authors [19], this option was not considered here. Spatial averaged mean square pressures were obtained directly from the linear Euler's equation. In addition, the transmission loss parameters obtained from the modal and classical approaches [6,11] were compared graphically as a function of frequency.

The results are organized as follows. Influence of panel positions (Figure 2) on SRI is discussed in section 4.2. Three and five different positions have been considered for the model 1 and for the model 2 respectively. Moreover, the simulation is compared with the Leppington's prediction [11] and with the field-incidence mass law theory [6]. In section 4.3, effects of the noise source placed in strategic points (Figure 1) in the source room are also compared. In the section 4.4, the depth of the source room (in both models) is increased by a factor of 2.5. The absorption surfaces were kept with the same area. Therefore, the cut-off frequencies of the room were only altered by the geometrical changes. In real buildings, the flat floor is normally divided into rooms, with the same height. Finally, in section 5, the influence of increase of absorption on two walls, the common wall surface and its opposite one, and of internal damping in the flexible partition are discussed.

4.2 - Influence of Panel Position on the SRI parameter

For the model 1, differences up to 30 dB at frequencies below 50 Hz have been observed between SRI curves for different panel positions. As the panel was moved into the center, its fundamental coupled frequency (table 4) was slightly changed and approximated to the first resonance frequencies of both rooms (table 1). Thus, a distinct dip in the SRI curve was

verified (Figure 9, 10). The phenomenon may be called 'coincidence'. In this situation, as the impedances of both rooms tended to an infinite value, the panel velocity amplitude tended to zero. In addition, at room resonance, the SRI is not dependent on the panel impedance, but on the panel position. In that case, the 'direct' geometrical coupling between rooms, thorough the 'opening' (panel of zero mass and zero stiffness) has been dominant. Above 100 Hz, the variation has remained at about 15 dB. On the other hand, at panel resonance, SRI was not dependent on the room impedance, but upon the geometrical coupling factors (Figure 4).

For the model 2, slight variations of SRI for different panel positions have been observed at frequencies below 75 Hz. This phenomenon may be explained by the fact that at low frequencies, the spatial distribution of the room modes varied slightly in **z** direction. Therefore, a smooth displacement of the panel along this axis did not have considerable influence on the noise insulation.

Between 75 Hz and 100 Hz, a variation of about 15 dB occurred at position 5. This may be justified by the fact that the position 5 is rather close to the nodes of the anti-symmetric room modes.

Finally, above 150 Hz, the panel at the centre of the common wall exhibited the best condition in terms of insulation. In that frequency range, the wavelength of the waves assumed values less than the heights of the rooms. The geometry of the 'corridor' in that situation had no influence on the interaction between modes. In other words, the system behaved like two similar rooms. Therefore, at the center, a better condition was found.

However, the SRI for the panel at position 2 was about 5 dB higher than the one at position 4. This may have occurred due to the ratio value between the source and receiving room dimension in the **z** direction. If the dimension ratio of the rooms in that direction were at least an integer value, the panel performance would tend to be quite similar at either position2 or at position 4.

In summary, the transmission behaviour has become complex and dependent on both the panel position and the panel size. Considering the panel located at the center of the common-wall, only few structural modes were excited. However, as the panel location was set at the corner of the wall, most of its even and odd modes were excited. This occurred because of the

response of a large number of *in vacuo* panel modes to oblique fields excited by the point source.

Another important point is that the fundamental structural mode was excited below the fundamental acoustic mode considering the whole wall. Thus, mass law controlled transmission was therefore dominant. However, for the small panel in the common wall, the first panel resonance frequency was located above the first acoustic resonance frequency, and a non-resonant stiffness behaviour was assumed (see Tables in section 7).

In Figure 9, SRI obtained from the Modal Analysis has been compared to that obtained by ref. [11] and infinite theory. The Predicted values, based on Leppington's analysis, were rather close to the one predicted by the mass law theory. This may be explained by the fact that the resonant terms of equation were negligible compared to the non-resonant contribution due to the low acoustic efficiency of the correspondent modes. It can also be seen that the SRI is inversely proportional to the panel size in the non-resonant transmission region. One observes that below the critical frequency, the effect of the panel size is significant when the whole wall is considered. Therefore, the curve for SRI tended to the mass-law curve.

4.3 - Influence of Source Position on the SRI parameter

In this analysis, the whole common wall is used in each model as the elastic structural partition. A point source has been placed at the positions shown in Figure 1. Values of SRI obtained for three different source positions are shown in Figure 6. The smoothest curve of SRI corresponds to the source located in the corner of the room, as it has been expected. With the source situated at the center of the room, only symmetric modes in the room were excited. The variation of source position produced differences up to 20 dB at the low-frequency range considered.

Most of the room modes were not excited at position 2 and the SRI curve has assumed high values. It is noted that at frequency band of 63 Hz, SRI was almost not affected by the source position. Below this frequency, in the middle of the room, sound insulation has achieved high values compared to the lower similar values obtained for the source placed at position 1 (corner) and 2. For a shallow source room shallow, similar modes were excited in both positions whereas in model 2 the SRI values differ due to the coupling with the cubic receiving room (Figure 6). However, a pronounced discrepancy among curves is verified

above 63 Hz. As noted in Figure 6, the three curves tend to coincide when the frequency have increased. This reveals that the reverberant sound field was quickly becoming diffuse.

In addition, the performance of the panel insulation has also been affected by the power input into the source room. It is also evident that the source position did not alter the coupling factors between the modes of the subsystems [21]

4.4 - Influence of Source Room Dimensions on the SRI parameter

The depth of the source room (**x** direction) was modified from 2 m to 5 m in both models. The results show that for the model 1 the SRI value varies of by about 10 dB and for the model 2 it varies of by about 20 dB. The SRI curve becomes smoother when the room depth of the source room is altered. However, for the small panel located at position 1 (at the corner), both models exhibit a significant variation when the depth dimension is altered. This can be explained by the fact that similar rooms are strongly coupled at the interface (common wall) due to their identical acoustic mode shapes. Alternatively, for a system composed by rooms of different volumes (model 2), a higher sound insulation is obtained. These situations might also be described in terms of acoustic impedance mismatching of the rooms. Thus, for a small panel, a high variation can be seen (Figure 7) at frequencies below 100 Hz.

In the following results, it might be verified that a change in the fundamental resonance frequency of the source room, by altering its depth, is crucial. Two types of acoustic modes, panel-controlled mode and room-controlled mode might be especially influenced by the interaction between them at low frequencies.

4.5 - Influence of internal loss factor and absorption on the SRI parameter

The SRI peak levels, shown in Figure 8, have been determined by the geometric modal coupling as well as by the damping factors at the resonant frequencies of the coupled system. As the modal overlap of the rooms was rather low, the cross-modal damping terms (equation 3.4) were neglected. In spite of that, the cross-modal terms of the radiation efficiency matrix dominate the resonant contribution, providing that the air is considered a 'light' fluid. [11]. In fact, mechanical damping is usually quite larger than the radiation damping. In addition, the effect of the panel internal loss factor has been more pronounced for the small panel than for the whole wall. In Figure 8, it is shown that its effect is negligible for the both models as the whole wall is considered.

According to Figure 5, the effect of the absorbing material at shifting the uncoupled structural natural frequencies has been negligible. On the other hand, the effect of increasing the absorption in the receiving room has significantly affected the SRI. For instance, when the reverberation time is decreased, the modal overlap factor is increased and vice-versa. Therefore, there is a higher probability of better coupling between modes with distinct eigenfrequencies. In both models, an increase in absorption led not only to better coupling but also to lower sound insulation. Material properties considered here were extracted from ref. [6] and [18]. The absorption coefficients for the volume surface were chosen as an averaged value of 0.05 (live rooms) over the whole frequency range.

4.6 – Coupling coefficients

Considering that the structural-acoustic coupling characteristics of the model room-plate-room are quite complex, all modes have been considered rather than selecting only those which have large contributions. In such case, this procedure might be justified by the results shown in Fig. 4 for the model 2. Even though there were many 'weakly coupling coefficients', their summation might be significant to the total coupling.

The geometrical coupling values have been obtained according to equation *3.2*. However, when an acoustic mode has coincided with a structural one, the geometrical coupling coefficients has been set to zero. Furthermore, these coefficients were normalized by their maximum absolute value in order to compare both models. According to the results, the relationship between the uncoupled structural and acoustic mode shape functions has shown large values at the lower order modes. This was evident at the lower acoustic and structural modes and when the room natural frequencies approximated to the panel natural frequencies. In addition, systems have shown negligible coupling effect if the lowest natural frequency of the uncoupled structural mode is substantially higher than that of the uncoupled acoustic mode.

4.7 – Ratio of Energy radiated into rooms.

In Figure 11, the ratio of the energy radiated into the source room to the energy radiated into the receiving room is shown. According to the results, it should be emphasized that the ratio variation for the model 1 is less pronounced than that for the model 2. It has confirmed the importance of the difference between the acoustic impedances of the coupled rooms on the SRI.

5 Conclusions

Comparison among the numerical modal analysis and the theoretical predictions has been performed. A narrow bandwidth (1 Hz) and a maximum frequency (350 Hz) were used for the models. Above this frequency limit, the computational storage requirements for variables as well as the operational running time became a large and complex problem to be determined by a personal computer. At the expensive of some complexity, the program might be extended to large problems by developing additional routines. Moreover, all possible natural frequencies and their respectively modes have been included in this analysis.

Then, it has been verified that Leppington's prediction is the one which approaches the values obtained via infinite theory when the non-resonant transmission is characterized.

These results may help the understanding of the model, as a group of subsystems directly related to physical elements such as rooms and flexible partitions. Also, they can provide an initial discussion for the investigation of a SEA model, which can be useful on practical building acoustics.

Although this problem, coupling between the panel and the acoustic fields, has been solved in previous work by several authors, the main originality of this initial research is to offer guidance on the comprehension of important parameters in a real case of architectural acoustic design. Nevertheless, this is yet to be validated experimentally.

In summary, all parameters, which have affected the modal composition of the sound field in the subsystems, were fundamental in the determination of the Sound Reduction Index. The results may also be used to predict measurement in-situ at low frequencies, where the classical definition of SRI in ISO140 for diffuse sound fields can not be reliable.

6 References

1. Dowell, E. H., Gorman, G. F., III and Smith, D. A., *Acoustoelasticity: General Theory, Acoustic Natural Modes and Forced response to Sinusoidal Excitation, Including Comparisons with Experiment*, Journal of Sound and Vibration, vol. 52(4), pp. 519-542, 1977.
2. Pan, J., Hansen, C. H. & Bies, D. A., *Active Control of Noise transmission Through a Panel into a Cavity: I. Analytical Study,* J. Acoust. Soc. Am. vol 87(5), pp. 2098-2108, 1990.
3. Kim, S. M. & Brennan M. J., *A Compact Matrix Formulation Using the Impedance and Mobility Approach for the Analysis of Structural-Acoustic Systems*, Journal of Sound and Vibration, vol. 223(1), pp. 97-113, 1999.
4. Fahy, F. J., *Sound and Structural Vibration*, Academic Press, U.K., 1995.
5. Fahy, F. J. & Mohammed, A. D., *A Study of Uncertainty in Applications of SEA to Coupled Beam and Plate Systems, Part I: Computational Experiments,* Journal of Sound and Vibration, vol. 158(1), pp. 45-67, 1992.
6. Beranek, L. L. & Vér, I. L., *Noise and Vibration Control Engineering,* John wiley & Sons, Inc. USA, 1992.
7. A. D. Pierce, *Acoustics: An Introduction to its Physical Principles and Applications,* New York: McGraw-Hill, 1981.
8. Brekke, A., *Calculation Methods for the Transmission Loss of Single, Double and Triple Partitions*, Applied Acoustics, vol. 14, pp. 225-240, 1981.
9. Fahy, F. J., *Statistical energy analysis. In Noise & Vibration* , ed. R. G. White & J. G. Walker. Ellis Horwood, Chichester, UK, chap.7, 1982.
10. Leppington, F., Broadbent, E., & Heron, K., *The acoustic radiation efficiency of rectangular panels,* Proc. Roy. Soc. Lond., A 382, pp. 245-271, 1982.
11. Leppington, F.G., Heron, K. H., Broadbent, F. R. S., & Mead, S. M., *Resonant and Non-Resonant Acoustic Properties of elastic Panels. II. The transmission Problem,* Proc. Roy. Soc. Lond., A 412, pp. 309-337, 1987.
12. Cremer, L., Heckl, M., & Ungar, E., *Structure-Borne Sound,* 2nd ed., Springer-Verlag, 1983.
13. Sewell, E. C., *Transmission of reverberant sound through a single-leaf partition surrounded by an infinite rigid baffle,* J. Sound Vib. 12(1), pp. 21-32, 1970.

14. White, F. M.; *Fluid Mechanics*, McGraw-Hill International Editions, Fourth Edition, Singapore, 1999.
15. Maidanik, G.; *Response of Ribbed Panels to Reverberant Acoustic Fields,* J. Acoust. Soc. Am.; vol 34, no. 6, pp. 809-826, 1962.
16. Takahashi, D.; *Effects of panel boundedness on sound transmission problems;* J. Acoust. Soc. Am. 98(5), pp. 2598-2606, 1995.
17. Osipov, A., Mess, P. and Vermeir, G.; *Low-Frequency Airborne Sound Transmission Through Single Partitions in Buildings;* Applied Acoustics, vol. 52, no. 3-4, pp. 273-288, 1997.
18. Gagliardini, L. & Roland, J.; *The Use of a Functional Basis to Calculate Acoustic Transmission Between Rooms;* Journal of Sound Vib. 145(3), pp. 457-458, 1991.
19. Guy, R. W. & Bhattacharya; *The transmission of sound through a cavity-backed finite plate;* Journal of Sound and Vibration , 27(2) pp. 207-223, 1973.
20. Kroop, W; Pietrzyk, A. & Kihlman, T. *On the meaning of the sound reduction index at low frequencies,* Acta Acustica 2, pp. 379-392, 1994.
21. Maluski, S. and Gibbs, B. , *The influence of partition boundary conditions on sound level difference between rooms at low frequencies,* Euro noise 98, pp. 681-685, 1998.
22. Maluski, S. and Gibbs, B.; *Sound Insulation between dwellings at low frequencies using a Finite Element Method.* Por. I. O. A. vol22, part 2, 2000.

7 Tables

Resonance frequencies of the first 20 uncoupled room modes – Model 1 and Model 2 Total number of modes of Room model 1 = 130 (0 - 350 Hz) Total number of modes of Room model 2 = 53 (0 – 350 Hz)			
Room Model 1 Mode (l,m,n) (2x2x5) m^3	Uncoupled resonance frequency (Hz)	Room Model 2 Mode (l,m,n) (2x2x2) m^3	Uncoupled resonance frequency (Hz)
0 0 1	34.00	0 0 1	85.00
0 0 2	68.00	0 1 0	85.00
0 1 0	85.00	1 0 0	85.00
1 0 0	85.00	0 1 1	120.21
0 1 1	91.55	1 0 1	120.21
1 0 1	91.55	1 1 0	120.21
0 0 3	102.00	1 1 1	147.22
0 1 2	108.85	0 0 2	170.00
1 0 2	108.85	0 2 0	170.00
1 1 0	120.21	2 0 0	170.00
1 1 1	124.92	0 1 2	190.07
0 1 3	132.77	0 2 1	190.07
1 0 3	132.77	1 0 2	190.07
0 0 4	136.00	1 2 0	190.07
1 1 2	138.11	2 0 1	190.07
1 1 3	157.65	2 1 0	190.07
0 1 4	160.38	1 1 2	208.21
1 0 4	160.38	1 2 1	208.21
0 0 5	170.00	2 1 1	208.21
0 2 0	170.00	0 2 2	240.42

Table 1: Summary of the resonance frequencies of the first twenty room modes

Panel modes Dimension: (1x1) m^2 Number of modes = 11 (0 – 350 Hz)		First 20 panel modes Dimension:(2x2) m^2 Number of modes = 52 (0 – 350 Hz)		First 20 panel modes Dimension: (2x5) m^2 Number of modes = 133 (0 – 350 Hz)	
Mode (p,q)	*In vacuo* natural frequency (Hz)	Mode (p,q)	*In vacuo* natural frequency (Hz)	Mode (p,q)	*In vacuo* natural frequency (Hz)
1 1	37.53	1 1	9.38	1 1	5.44
1 2	93.82	1 2	23.45	1 2	7.69
1 3	93.82	1 3	23.45	2 1	11.44
1 4	150.12	1 4	37.53	2 2	16.70
2 1	187.64	2 1	46.91	1 3	19.51
2 2	187.64	2 2	46.91	3 1	21.77
1 5	243.94	1 5	60.98	2 3	23.46
2 3	243.94	2 3	60.98	3 2	25.52
2 4	318.99	2 4	79.75	1 4	30.77
1 6	318.99	1 6	79.75	4 1	31.71
2 5	337.76	2 5	84.43	3 3	37.53
-	-	1 7	93.82	2 4	41.47
-	-	3 1	93.82	4 2	42.97
-	-	3 2	117.28	3 4	45.22
-	-	2 6	117.28	4 3	45.79
-	-	3 3	121.97	1 5	48.98
-	-	1 8	121.97	5 1	52.73
-	-	3 4	136.04	2 5	54.23
-	-	2 7	136.04	5 2	55.54
-	-	3 5	150.12	4 4	60.98

Table 2: Summary of the *in vacuo* natural frequencies of the flexible panels used in he models.

First 20 resonance frequencies of the model 1- Panel dimension: (2 x 5) m^2 Number of modes of the panel = 133		First 20 resonance frequencies of the model 2 Panel dimension: (2 x 2) m^2 Number of modes of the panel = 52	
Coupled frequency (Hz)	Coupled frequency* (damping included) (Hz)	Coupled frequency (Hz)	Coupled frequency* (damping included) (Hz)
5.28	-0.0257+ 5.2777i	9.03	-0.0445 + 9.0321i
7.19	-0.0354 + 7.1896i	22.95	-0.1138 +22.9507i
11.12	-0.0544 +11.1216i	22.97	-0.1135 +22.9692i
16.26	-0.0811 +16.2632i	34.36	-0.4694 +34.3575i
19.07	-0.0939 +19.0680i	37.06	-0.1839 +37.0568i
21.33	-0.1053 +21.3340i	46.48	-0.2347 +46.4848i
23.09	-0.1141 +23.0934i	46.49	-0.2310 +46.4949i
25.11	-0.1241 +25.1014i	60.46	-0.3020 +60.4606i
30.37	-0.1504 +30.3677i	60.49	-0.3017 +60.4959i
31.03	-0.1718 +31.0299i	68.13	-0.4723 +68.1250i
34.00	-0.4735 +33.9967i	78.84	-0.4049 +78.8429i
35.78	-0.4430 +35.7750i	79.05	-0.4055 +79.0462i
37.12	-0.1842 +37.1245i	83.89	-0.4364 +83.8876i
41.08	-0.2041 +41.0751i	85.00	-0.6040 +84.9992i
42.47	-0.2109 +42.4686i	85.00	-0.6039 +85.0001i
45.07	-0.2345 +45.0659i	85.66	-0.6675 +85.6550i
45.40	-0.2257 +45.4064i	85.86	-0.6390 +85.8607i
48.45	-0.2411 +48.4490i	86.28	-0.6305 +86.2738i
52.00	-0.2622 +52.4291i	91.73	-0.6327 +91.7269i
53.83	-0.2683 +53.8342i	92.02	-0.6421 +92.0174i

Table 3: Summary of the first 20 resonance frequencies of model 1 and 2

* - Imaginary part of the values

Resonance frequencies of the model 1 - Panel dimension: (1 x 1) m^2					
F_{c1} (Hz)	F_{dc1}^* (Hz)	F_{c2} (Hz)	F_{dc2}^* (Hz)	F_{c3} (Hz)	F_{dc3}^* (Hz)
32.84	-0.3872 +32.8373i	33.50	-0.4279 +33.4952i	34.00	-0.4734 +33.9954i
34.00	-0.4735 +33.9967i	34.00	-0.4735 +33.9967i	34.00	-0.4735 +33.9967i
38.04	-0.2686 +38.0397i	37.62	-0.2297 +37.6208i	37.09	-0.1848 +37.0917i
68.00	-0.4735 +67.9984i	68.00	-0.4735 +67.9984i	68.00	-0.4735 +67.9984i
68.13	-0.4736 +68.1272i	68.00	-0.4733 +68.0022i	68.21	-0.4738 +68.2118i
84.97	-0.5740 +84.9633i	84.93	-0.5731 +84.9259i	84.91	-0.5726 +84.9057i
85.00	-0.5749 +84.9981i	85.00	-0.5749 +84.9981i	85.00	-0.5749 +84.9981i
85.00	-0.5749 +84.9981i	85.00	-0.5749 +84.9981i	85.00	-0.5749 +84.9981i
85.20	-0.5752 +85.1994i	85.17	-0.5752 +85.1658i	85.16	-0.5752 +85.1563i
91.25	-0.6136 +91.2495i	91.34	-0.6239 +91.3360i	91.41	-0.6301 +91.4121i
91.55	-0.6426 +91.5455i	91.55	-0.6426 +91.5455i	91.55	-0.6426 +91.5450i

Table 4: Summary of the resonance frequencies of the panel (1x1) m^2 at positions 1, 2 and 3- Resonance frequencies: F_c - coupled freq. (without damping); F_{dc} - coupled modes with damping;

* - Imaginary part of the values

Resonance frequencies of the model 2 - Panel dimension: (1 x 1) m^2 -									
F_{c1} (Hz)	F_{dc1}^* (Hz)	F_{c2} (Hz)	F_{dc2}* (Hz)	F_{c3} (Hz)	F_{dc3}^* (Hz)	F_{c4} (Hz)	F_{dc4}^* (Hz)	F_{c5} (Hz)	F_{dc5}^* (Hz)
33.33	-0.4133 +33.3265i	33.43	-0.4239 +33.4343i	33.54	-0.4323 +33.5359i	33.62	-0.4378 +33.6234i	33.71	-0.4432 +33.7117i
37.49	-0.2429 +37.4898i	37.71	-0.2344 +37.7078i	37.76	-0.2271 +37.7591i	37.52	-0.2205 +37.5208i	37.15	-0.2133 +37.1442i
68.06	-0.4736 +68.0622i	68.03	-0.4735 +68.0291i	68.00	-0.4734 +68.0004i	67.99	-0.4734 +67.9893i	68.00	-0.4734 +67.9998i
84.93	-0.6678 +84.9360i	84.87	-0.6517 +84.8861i	84.84	-0.6458 +84.8514i	84.87	-0.6519 +84.8865i	84.93	-0.6679 +84.9364i
84.96	-0.6720 +84.9631i	84.91	-0.6703 +84.9088i	84.89	-0.6721 +84.8843i	84.91	-0.6703 +84.9090i	84.96	-0.6721 +84.9634i
85.00	-0.5822 +84.9833i	84.91	-0.5968 +84.9819i	85.00	-0.6000 +84.9849i	85.00	-0.5968 +84.9819i	85.00	-0.5821 +84.9834i
85.00	-0.6002 +84.9998i	85.00	-0.6025 +85.0035i	85.00	-0.6028 +85.0055i	85.00	-0.6025 +85.0035i	85.00	-0.6002 +84.9997i
85.44	-0.6522 +85.4312i	85.00	-0.6497 +85.3074i	85.27	-0.6489 +85.2642i	85.32	-0.6497 +85.3082i	85.44	-0.6521 +85.4372i
91.39	-0.6255 +91.3886i	85.32	-0.6243 +91.3242i	91.33	-0.6257 +91.3289i	91.40	-0.6300 +91.4008i	91.47	-0.6325 +91.4717i
91.69	-0.6397 +91.6892i	91.33	-0.6409 +91.6494i	91.62	-0.6404 +91.6165i	91.59	-0.6390 +91.5836i	91.55	-0.6372 +91.5436i
93.18	-0.4680 +93.1830i	91.65	-0.4721 +93.5117i	93.62	-0.4737 +93.6164i	93.76	-0.4741 +93.5635i	93.34	-0.4711 +93.3345i

Table 5: Summary of the resonance frequencies of the model 2. Panel (1x1) m^2 at positions 1, 2, 3, 4, and 5 - Resonance frequencies: F_c – coupled modes without damping; F_{dc} – coupled modes with damping;

* - Imaginary part of the values

8 Figures

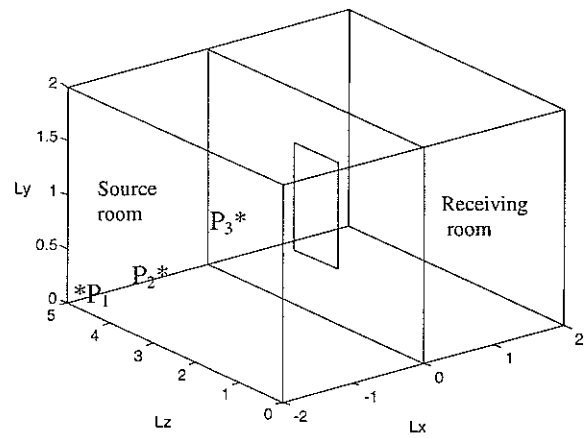

Figure 1: Two rooms separated by a common wall with a centered flexible panel.
Coordinates of the point sources :P_1 = (2,0,0) – at the corner ;P_2 = (1,0,0)
P_3 = (1,1,2.5) – In the middle of the room

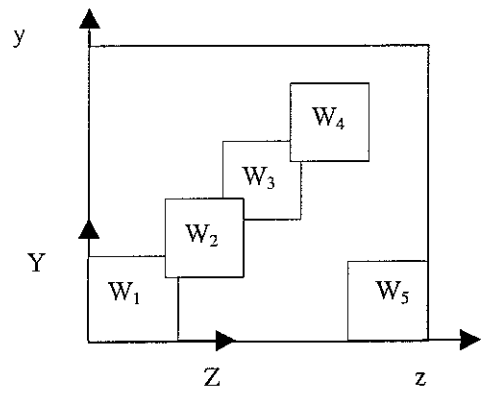

Figure 2: Different positions for the flexible panel in the wall.
Coordinates (Z,Y) of the panel position : Model 1:W_1 = (0,0); W_2 = (1,0.25); W_3 = (2,0.5)
Model 2: W_1 = (0,0); W_2 = (0.25,0.25); W_3 = (0.5,0.5); W_4 = (0.75,0.75); W_3 = (1,0);

MODEL 1

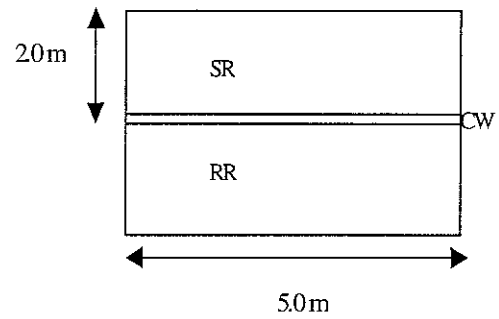

MODEL 2

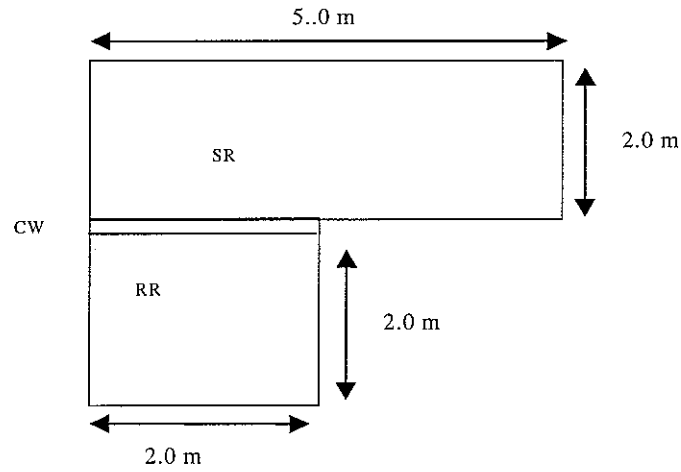

Figure 3: Room plan shapes; RR (Receiving room); SR (Source room); CW (Common wall)

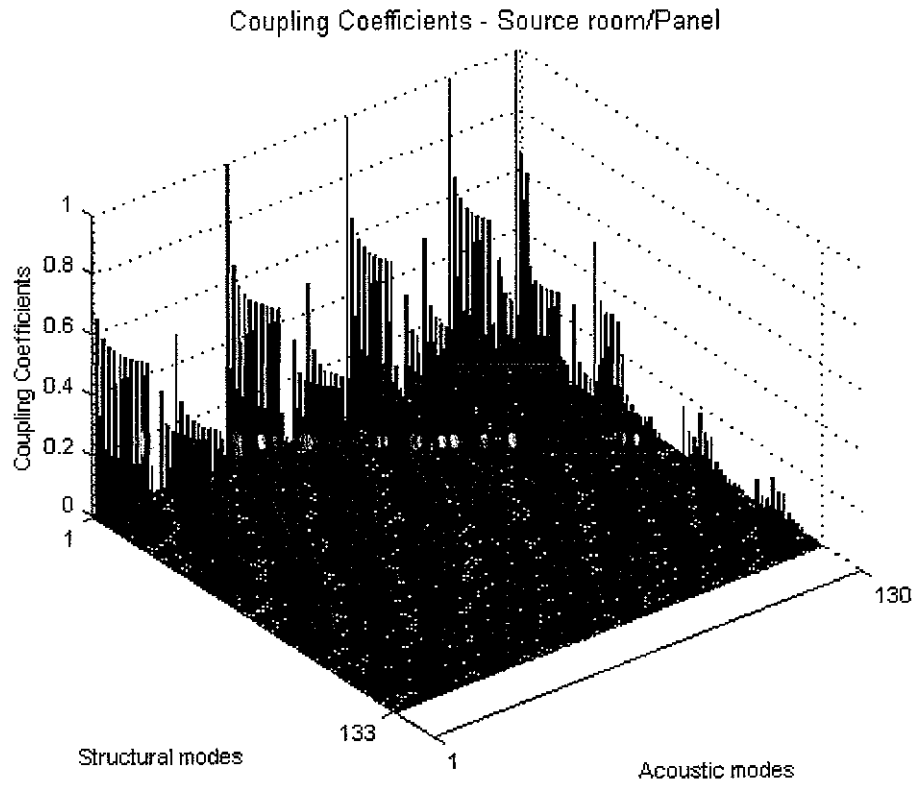

Figure 4 a – Normalised geometric coupling coefficients to maximum of unity – Model 1

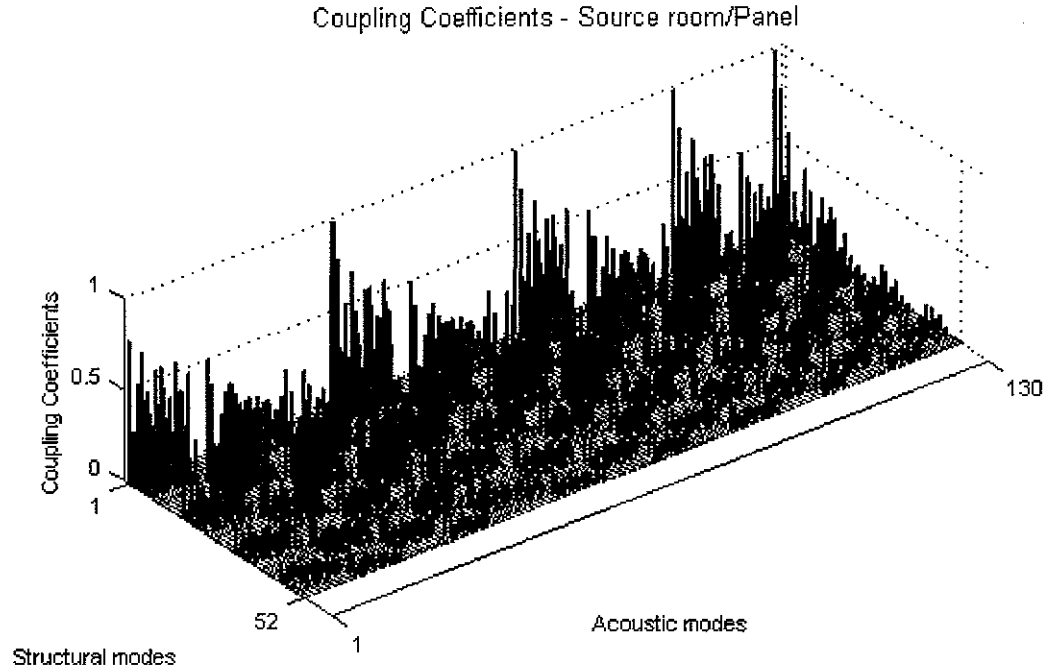

Figure 4 b – Normalised geometric coupling coefficients to maximum of unity – Model 2

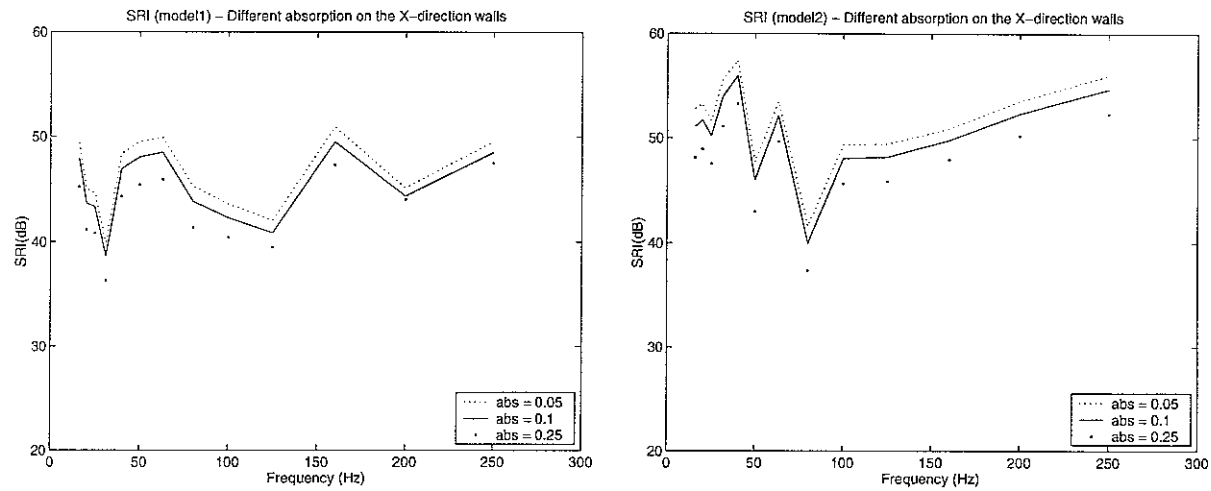

Figure 5 – The influence of room absorption on the SRI curve for the whole wall. (one-third frequency band)

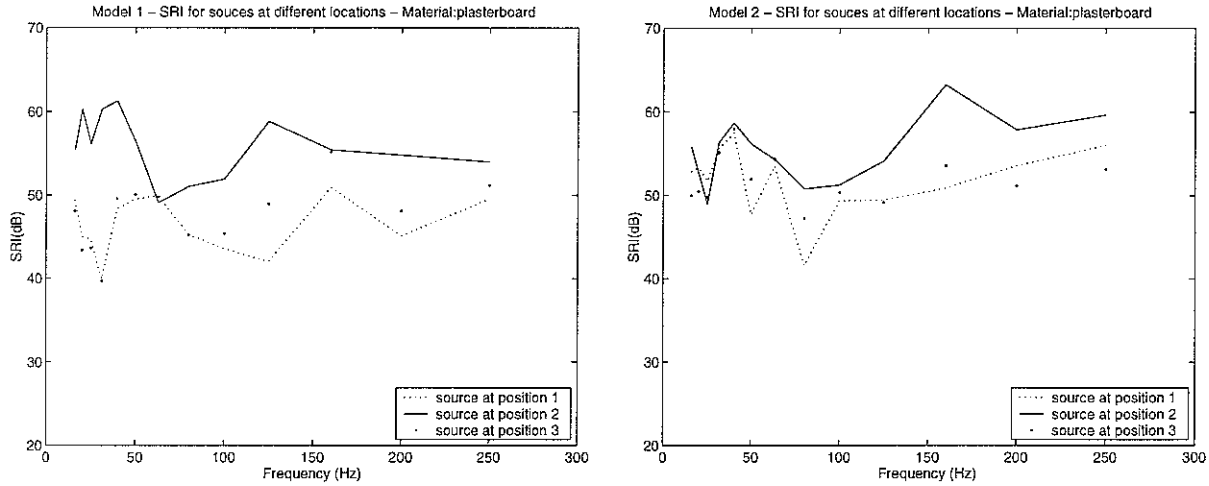

Figure 6 – The influence of Source Position on the SRI curve for Model 1 and 2 (whole wall). (one-third frequency band)

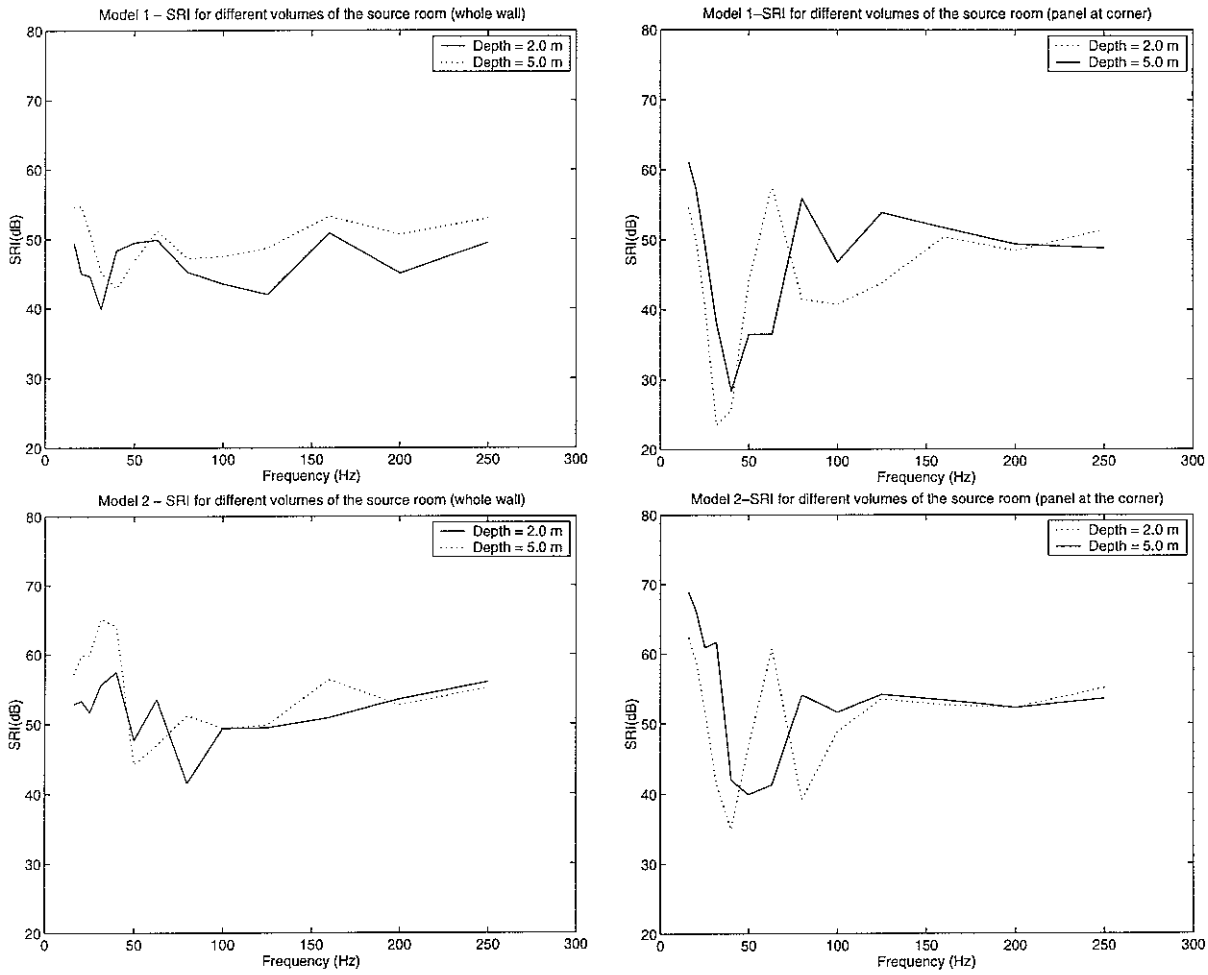

Figure 7 – The influence of source room dimensions on the SRI curve for Models 1 and 2. (one-third frequency band)

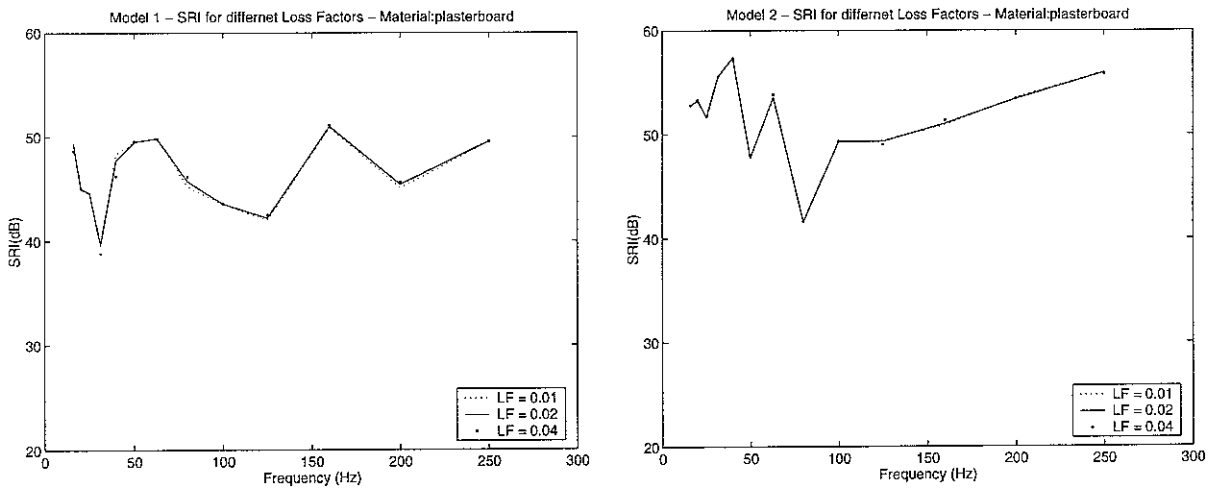

Figure 8 – The influence of panel internal loss factor on the SRI curve for Models 1 and 2. (one -third frequency band)

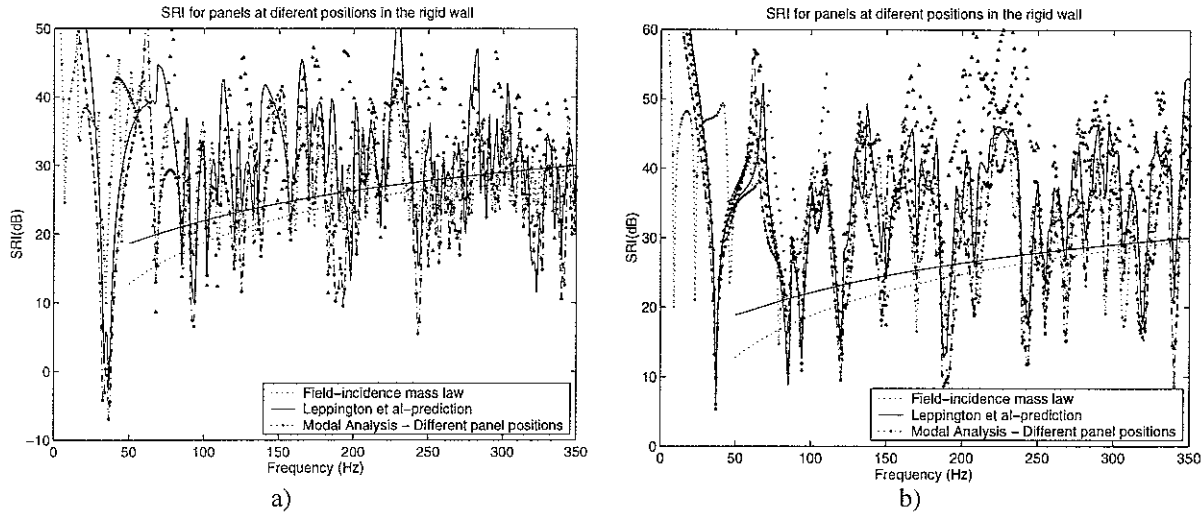

Figure 9 – SRI curve for comparison between Modal Analysis and others. a) model 1; b) model 2 (Narrowband)

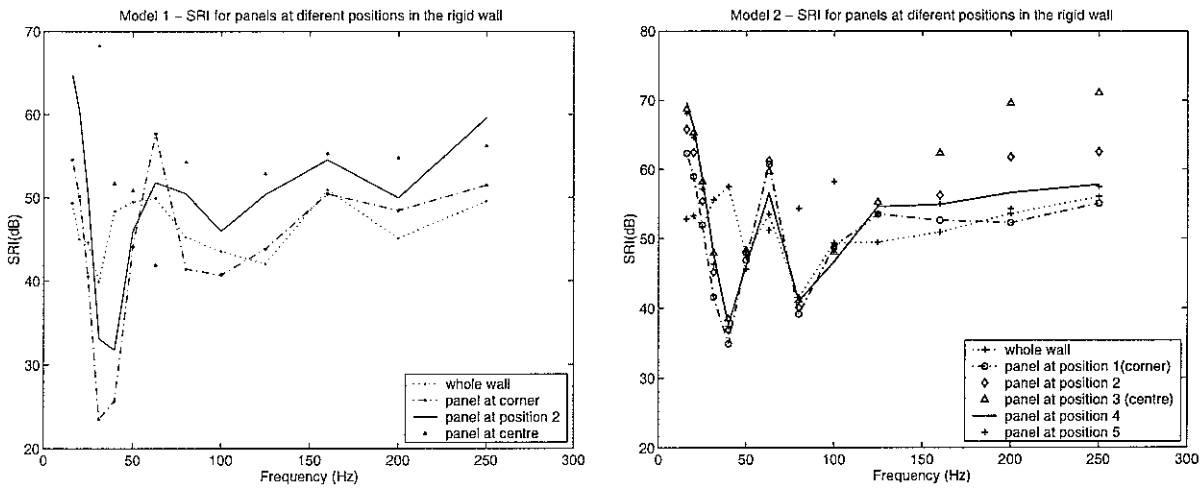

Figure 10 – The influence of Panel Position on the SRI curve. (one-third frequency band)

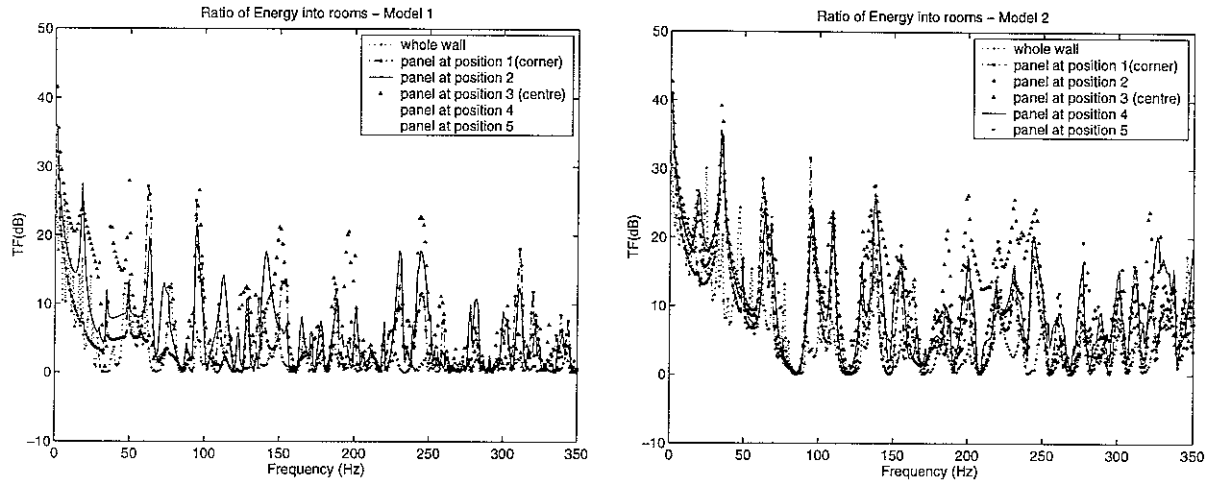

Figure 11 – Ratio of energy radiated into the source room to the energy radiated into the receiving room; (Narrowband frequencies)

9 Appendix

List of symbols

$\mathbf{c_o}$ - ambient (equilibrium) speed of sound;

$\mathbf{p(z,y,0)}$ - Pressure over the panel surface;

$\mathbf{k_z}$ - trace wavelength of the panel at the z direction;

$\mathbf{k_y}$ - trace wavelength of the panel at the y direction;

$\mathbf{k_b}$ - trace wavelength of free-bending waves propagating in a infinite panel;

$\mathbf{k_{pr}}$ - trace wavelength of the panel *in vacuo*;

w - normal displacement of the panel surface;

$\mathbf{C_{n1p}}$ - geometrical coupling between the source room and the panel;

$\mathbf{C_{n2p}}$ - geometrical coupling between the receiving room and the panel;

$\mathbf{F_n^R}$ - generalized force exerted on the p^{th} plate mode by the n^{th} acoustic mode of the receiving room;

$\mathbf{G(r \mid r_o)}$ - Green's Function – solution to equation (2.14);

$\mathbf{P_n^R}$ - receiving room modal pressure;

$\mathbf{Q_n}$ - generalized volume velocity; see equation (3.3);

$\mathbf{Z_a}$ - real specific acoustic impedance; see equation (3.5);

α - constant diffuse absorption coefficient;

β_p, β_n, - Modal damping parameter of the panel and of the acoustic space respectively;

ϕ_p , ϕ_q - function basis for the eigenfunctions of a simply-supported plate;

η - Internal loss factor;

ρ_o - density of air (equilibrium);

τ - transmission efficiency – see equation (2.1);

ω - forced angular frequency;

ψ_n - function basis for the mode shapes of an acoustic volume boundary by rigid walls;

$\Pi(\omega)$ - Power radiated into a half-space due to the plate vibration in the frequency domain;

∇ - Laplace's operator;

$\Phi_{n1,n2}$ - Potential velocity function corresponding to the source and receiving rooms;

Λ_p - Generalized modal mass for the panel;

Λ_n - Generalized modal mass for the the acoustic volume;